FE-2729-7
Distribution Category UC-90c

ALLOY CATALYSTS WITH MONOLITH SUPPORTS FOR METHANATION OF COAL-DERIVED GASES

Quarterly Technical Progress Report
For Period March 21, 1979 to June 20, 1979

Calvin H. Bartholomew
Brigham Young University
Provo, Utah 84602

Date Published -- July 5, 1979

PREPARED FOR THE UNITED STATES
DEPARTMENT OF ENERGY

Under Contract No. EF-77-S-01-2729

MASTER

Blank Page

FOREWORD

This report summarizes technical progress during the seventh quarter (March 21, 1979 to June 20, 1979) of a two-year study conducted for the Department of Energy (DOE) under Contract No. EF-77-S-01-2729. The principal investigator for this work was Dr. Calvin H. Bartholomew; Dr. Paul Scott was the technical representative for DOE.

The following students contributed to the technical accomplishments and to this report: Erek Erekson, Ed Sughrue, Gordon Weatherbee, Don Mustard, and John Watkins. Mr. Erekson and Dr. Bartholomew were the principal authors. April Washburn and Steve Kvalve provided typing and drafting services. In this report data are reported in SI units.

TABLE OF CONTENTS

LIST OF FIGURES

LIST OF TABLES

ABSTRACT

During the seventh quarter significant progress was made in several task areas, but especially in the investigations of high pressure kinetics and deactivation by sulfur poisoning. Seventeen new catalysts were prepared for use in kinetic studies and long term tests. A number of catalysts were characterized using H_2 and CO adsorption and transmission electron microscopy. Activity tests were conducted for a borohydride reduced catalyst and samples of crushed and uncrushed monolithic nickel catalyst. Extensive kinetic experiments were performed on two monolithic nickel catalysts over a range of temperatures and pressures from which kinetic parameters and a rate expression were obtained. Long term experiments of H_2S poisoning during reaction were also conducted and the data were fitted to a Levenspiel deactivation kinetics model. The principal investigator visited three other laboratories and presented a paper at the Catalysis Gordon Conference.

I. OBJECTIVES AND SCOPE

A. Background

Natural gas is a highly desirable fuel because of its high heating value and nonpolluting combustion products. In view of the expanding demand for and depletion of domestic supplies of clean fuels, economic production of synthetic natural gas (SNG) from coal ranks high on the list of national priorities.

Presently there are several gasification processes under development directed toward the production of SNG. Although catalytic methanation of coal synthesis gas is an important cost item in each process, basic technological and design principles for this step are not well advanced. Extensive research and development are needed before the process can realize economical, reliable operation. Specifically, there appear to be important economical advantages in the development of more efficient, stable catalysts.

From the literature (1,2), three major catalyst problems are apparent which relate to stability: (i) sulfur poisoning, (ii) carbon deposition with associated plugging, and (iii) sintering. Our understanding of these problems is at best sorely inadequate, and the need to develop new and better catalyst technology is obvious. Nevertheless, there has been very little research dealing with new catalyst concepts such as bimetallic (alloy) or monolithic-supported catalysts for methanation. This study deals specifically with sulfur poisoning, carbon deposition, and the effects of support (monolith and pellet) geometry on the performance of alloy methanation catalysts.

B. Objectives

The general objectives of this research program are (i) to study the kinetics of methanation for a few selected catalysts tested during the first two years, (ii) to investigate these catalysts for resistance to deactivation due to sulfur poisoning and thermal degradation. The work is divided into five tasks.

Task 1. Characterize the surface, bulk and phase compositions, surface areas, and metal crystallite sizes for alumina-supported Ni, Ni-Co, Ni-MoO_3, Ni-Pt, Ni-Ru and Ru catalysts.

Task 2. Continue activity testing and support geometry studies of Ni and Ni-bimetallic catalysts initiated during the first two years. The tests include (i) conversion vs. temperature runs at low and high pressures, (ii) steady-state carbon deposition tests, (iii) in situ H_2S tolerance tests, and (iv) support geometry comparisons.

Task 3. Perform kinetic studies to find intrinsic rate data for alumina-supported Ni, Ni-Co, Ni-MoO_3, Ni-Pt, Ni-Ru, and Ru catalysts over a range of pressures and feed compositions. Detailed rate expressions for each catalyst will be determined at low and high pressure.

Effectiveness factors for monolithic and pellet-supported nickel on alumina will be obtained by comparing specific rates to those of finely powdered nickel on alumina.

Task 4. Determine H_2S poisoning rates, thermal deactivation rates, and operating temperature limits for Ni, Ni-Co, Ni-MoO_3, Ni-Pt, Ni-Ru, and Ru catalysts.

Task 5. Continue laboratory visits and technical communications. Interact closely with industrial and governmental representatives to promote large scale testing and development of the two or three best monolithic or pelleted alloy catalysts from this study.

C. Technical Approach

The technical approach which will be used to accomplish the tasks outlined above is presented in the statement of work dated May 20, 1977. The main features of that approach are reviewed here along with more specific details and modifications which have evolved as a result of progress. It is expected that various other aspects of this approach will be modified and improved as the project develops and as new data are made available. Nevertheless, the objectives, tasks and principle features of the approach will remain the substantially the same.

Task 1: Catalyst Characterization

A comprehensive examination of alumina-supported Ni, Ni-Co, Ni-MoO_3, Ni-Pt, Ni-Ru, and Ru catalysts will be carried out to determine surface, bulk, and phase compositions, surface areas, and metal crystallite sizes using the following techniques: chemisorption, x-ray diffraction, chemical analysis, ESCA and SIMS spectroscopy, Auger spectroscopy and transmission electron microscopy.

Hydrogen chemisorption uptakes will be measured using a conventional volumetric apparatus before each reactor test and before and after deactivation tests. X-ray diffraction measurements will be carried out to determine the active metallic phases and metal crystallite size where possible. Selected "aged" samples from Task 4 will be analyzed (by x-ray, chemical analysis, and perhaps ESCA) to determine carbon content and possible changes in phase composition or particle size. Also, transmission electron micrographs will be made to determine particle size distributions for catalyst samples. A few samples will be analyzed by EDAX to determine composition.

Task 2: Activity Testing and Support Geometry Design

Methanation activity and sulfur tolerance measurements initiated during the previous two years of study (3) will be completed. Pellet and monolithic alumina-supported Ni, Ni-Co, Ni-MoO_3, Ni-Pt, Ni-Ru, and Ru catalysts, (both high and low metal loadings) will be activity

tested over a range of temperatures, pressures, and H_2S concentrations. A comparison of steady state conversions for nickel on different pellet and monolith supports of varying geometry will be made. Low pressure activity and sulfur tolerance tests will also be made for pelleted Co/Al_2O_3 and unsupported Ni-Co and Ni-Mo alloys. A summary of the five test procedures and corresponding experimental conditions is listed in Table 1.

Task 3: Kinetic Studies

In order to make more extensive kinetic studies of the six catalyst metal combinations a new mixed flow reactor system will be constructed. This system will be capable of operation to 7500 kPa and 775 K and over a range of reactant compositions. The reactor for this system will be a "Berty" type constant volume mixed flow Autoclave reactor.

Intrinsic rate data will be obtained for alumina-supported Ni, Ni-Co, Ni-MoO_3, Ni-Pt, Ni-Ru, and Ru catalysts over a range of pressures and feed compositions in order to obtain detailed rate expressions at low and high pressures. To insure gradientless operation in the reaction-limited regime the rates will be measured at low conversions (0-5%) and low temperatures (525-600 K) for samples which have been crushed to obtain small particles.

Isothermal effectiveness factors for monolithic and pellet-supported nickel on alumina will be obtained by comparing their specific rates to those of finely powdered nickel on alumina using the same mixed flow reactor.

Task 4: Degradation Studies

H_2S poisoning rates and thermal deactivation rates at low pressure will be studied using a new quartz reactor system. Quartz was selected as the material for the reactor because it must operate at high temperatures (750-1000 K) and in a corrosive (H_2S) environment. This reactor is also a constant volume mixed flow type reactor according to the design of Katzer (4). The quartz reactor system will be constructed during the early part of the contract period. Thermal deactivation at high pressures will be studied using a tubular stainless steel reactor previously discussed (3).

Operating temperature limits (and specific reaction rates within this range), thermal deactivation rates near the upper use temperature (in the presence and absence of steam), and H_2S poisoning rates (at 525 K in the presence of 1 and 10 ppm H_2S in H_2) will be determined for Ni, Ni-Co, Ni-MoO_3, Ni-Pt, Ni-Ru, and Ru catalysts. The extent of carbon-carbide deposited in the thermal deactivation runs will be determined by chemical analysis and x-ray diffraction.

Table 1

Description of Reactor Tests for Task 2

Test Procedures	Experimental Conditions
1. Temperature-Conversion Test: Measure CO conversion and methane production as a function of temperature, with and without 1% (by vol.) of steam present in the reactant mixture.	475-675 K 140 kPa 30,000 hr^{-1} 1% CO, 4% H_2, 95% N_2 (dry basis)
2. Temperature-Conversion Test (high pressure): Measure CO conversion and methane production as a function of temperature at 2500 kPa.	475-675 K 2500 kPa 30,000 hr^{-1} 1% CO, 4% H_2, 95% N_2
3. Steady State (24 Hr.) Carbon Deposition Test: Measure CO conversion and methane production at 500 and 525 K (250,000 hr^{-1}) before and after an exposure of 24 hours at 675 K.	675 K (24 hrs.) 140 kPa 200,000-250,000 hr^{-1} 25% CO, 50% H_2, 25% N_2 $H_2/CO = 2$
4. In situ H_2S Tolerance Test: Measure intermittently the production of methane and hydrocarbons (by FID) during 24 hours exposure to feed containing 1 or 10 ppm H_2S using a glass reactor.	525 K 140 kPa 30,000 hr^{-1} 1% CO, 4% H_2, 95% N_2 1 or 10 ppm H_2S
5. Support Geometry Tests: Measure CO conversion and methane production as a function of temperature for the same Ni/Al_2O_3 catalyst supported on monoliths and pellets of varying geometries.	575-675 K 140 kPa 30,000 hr^{-1} 1% CO, 4% H_2, 95% N_2

Task 5: Technical Interaction and Technology Transfer

The principal investigator will continue to communicate closely with other workers in methanation catalysis, continue distribution of quarterly reports to selected laboratories to stimulate interest and feedback, attend important coal and catalysis meetings, and visit other methanation laboratories.

He will also interact closely with Mr. A.L. Lee at the Institute of Gas Technology, with personnel at the Pittsburgh Energy Research Center and with other coal gasification representatives to promote large scale testing and development of the two or three best catalysts from this study.

II. SUMMARY OF PROGRESS

A project progress summary is presented in Figure 1 and accomplishments during the past quarter are summarized below. Figure 1 shows that task accomplishments are on schedule.

Accomplishments and results from the past quarter are best summarized according to task:

Task 1. Fifteen monolithic supported and two pellet supported nickel catalysts were prepared for use in kinetic studies and long term tests. H_2 adsorption uptakes were measured for 7 different catalyst samples. Surface areas of several 3 wt.% Ni/monolithic catalysts were found to be comparable to those for 3% Ni/Al_2O_3 pellets. CO adsorption measurements were carried out at 273 and 298 K on fresh and presulfided samples of 3% Ni/Al_2O_3. CO uptake increased by factors of 3-8 after exposure to H_2S. Electron micrographs of 13.5% Ni/SiO_2 were obtained for freshly reduced and sintered samples. The average metal crystallite diameter determined by this technique is in very good agreement with that estimated from H_2 chemisorption.

Task 2. Initial specific intrinsic activity tests were performed on a borohydride reduced Ni_2B/Al_2O_3, the results showing its methane production rate (mass basis) to be slightly higher and its turnover number somewhat lower than 14% Ni/Al_2O_3. Activity tests performed on two samples of a monolithic catalyst (whole monolith and monolith crushed to a powder) resulted in the same turnover number within experiment error. These latter results suggest that differences observed previously for monolithic and pellet catalysts in similar tests were due to differences in intrinsic activity -- not in flow or diffusional characteristics.

Task 3. Extensive kinetic experiments were conducted with two monolithic nickel catalysts over a range of temperatures (200-275 K) and pressure (8-75 atm). From the data activation energies and concentration dependencies were obtained. These kinetic parameters are generally in good agreement with values obtained at ambient pressure, although the reaction orders for CO and H_2 vary with pressure and temperature conditions.

Task 4. Long term experiments of H_2S poisoning during reaction were conducted on samples of 3% Ni/Al_2O_3. Activity versus time curves were fitted to a Levenspiel deactivation kinetics model with varying degrees of success. After partial *in situ* poisoning the kinetics for methanation were not significantly altered.

Task 5. The principal investigator provided technical assistance to DOE in connection with the Three-Mile Nuclear Reactor accident. He visited IGT, the Ventron Corporation and The University of Delaware and presented a paper at the Catalysis Gordon Conference. Our Laboratory received two requests from companies for samples of our catalysts to be tested in methanation processes. A paper on sulfur poisoning was accepted for publication.

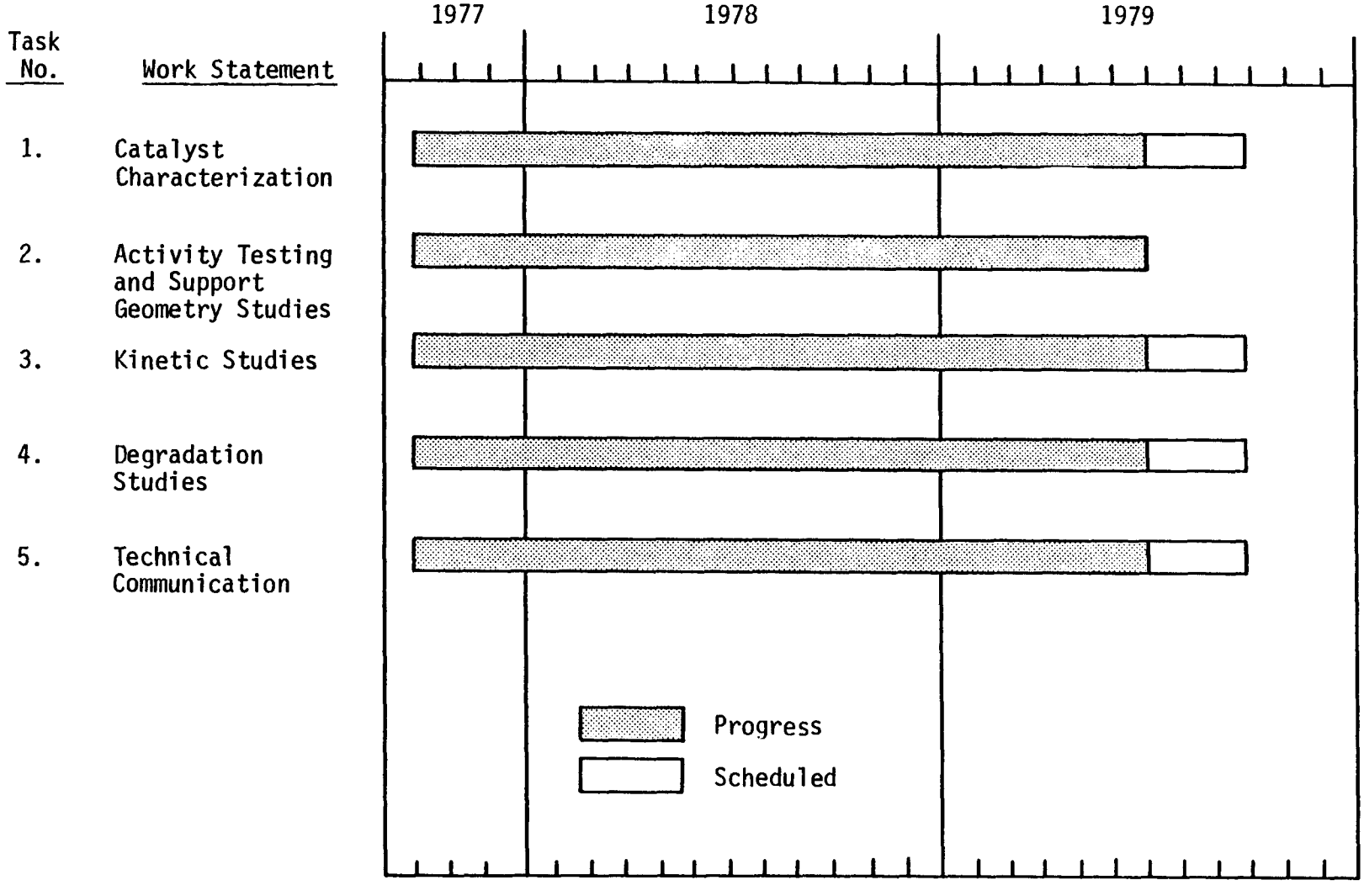

Figure 1. Project Progress Summary

III. DETAILED DESCRIPTION OF TECHNICAL PROGRESS

Task 1: Catalyst Characterization

1. Catalyst Preparation

During the past quarter the following catalysts were prepared: Ni-M-182 to 192, Ni-NAL-M-100 to 103, Ni-A-123 and Ni-NAL-101. Nominal compositions are listed in Table 2. The catalysts numbered Ni-M-182 to 187 are 3% nickel and 10% alumina on Corning monolithic cordierite supports. The series Ni-M-188 to 191 are a similar preparation but with only 0.5% nickel. The use of the 0.5% nickel monolithic should allow testing at higher temperatures. The Ni-A-123 catalyst is 4.3% nickel on Kaiser alumina pellets. This catalyst was prepared to compare metal/volume ratios with monoliths in high pressure kinetic studies.

The Ni-NAL-M-100-103 and the Ni-NAL-101 catalysts were prepared for Battelle Northwest. The Ni-NAL-M-100-103 are cordierite monoliths with 20% alumina and approximately 30% nickel. The Ni-NAL-101 is 30% nickel on Conoco's Catapal extrudates. In the preparation of all four of these catalysts approximately one-half of the Ni was reacted with alumina by means of calcination at 600°C to form a Ni Al_2O_4 support, which was subsequently impregnated with the remaining nickel.

2. Hydrogen Chemisorption Measurements

Hydrogen chemisorption measurements were performed on several catalyst samples. Data for these samples is listed in Table 3. Three samples of Ni-A-120 (3% Ni) pellets, +60 mesh powder, and -60 mesh powder are shown. While the H_2 uptakes vary by as much as 20%, this difference is within the experimental accuracy of the chemisorption technique ($\pm$ 10%). H_2 uptake values for several 3% Ni/monolith catalyst used in Task 3 are significantly higher than values obtained for the pellets. In other words, it is possible to obtain equivalent or even higher metal dispersions using coated monoliths.

3. Carbon Monoxide Chemisorption Measurements

During the past quarter, investigation of the formation of nickel carbonyl during CO chemisorption continued with the first testing of presulfided catalysts.

The experiments are performed using a standard powder catalyst reactor cell developed earlier (3). The catalyst is loaded into this cell and reduced for two hours in flowing hydrogen at 723 K and subsequently evacuated to a pressure of 7×10^{-6} kPa. The catalyst is then titrated with carbon monoxide as described in earlier reports (3,5), except that after each isotherm, the titration gas is evacuated through a coil of pyrex glass immersed in liquid nitrogen. In this way any $Ni(CO)_4$ or COS formed is frozen out on the inside of the coil. After the completion of the evacuation procedures, the coil is warmed to about 323 K volatilizing the carbonyls. These gases are carried out by a stream of high purity helium first through a small section of glass tubing heated to 500 K and are then allowed to bubble through a solution of cadmium acetate. The amount of nickel carbonyl formed

Table 2

Catalyst Composition Data

Catalyst	Nominal Composition (wt% nickel)	(wt% alumina)	Support
Ni-M-182 thru 187	3.0	10	Cordierite Monolith
Ni-M-188 thru 191	0.5	10	Cordierite Monolith
Ni-NAL-M-100 thru 103	30	20	Cordierite Monolith
Ni-A-123	4.3	95+	Kaiser Alumina Pellets
Ni-NAL-101	30	70	Catapal Extrudates

Table 3

H_2 Chemisorption Uptake Data

Catalyst	Nominal Composition (wt.% nickel)	H_2 Uptake (μmoles/gram)
Pellets		
Ni-A-120	3	31.0[a]
Powders		
Ni-A-120 -60 mesh	3	24.9
Ni-A-120 +60 mesh	3	29.0
Monoliths		
Ni-M-157	3	38.2
Ni-M-159	3	41.6
Ni-M-183	3	39.6
Ni-M-184	3	39.0

[a] Previously reported.

is determined by the increase in weight of the glass tube or alternately by means of atomic absorption analysis. The solution of cadmium acetate is titrated with an amine as described in earlier sulfur work (5) to determine the amount of COS formed (6).

Table 4 lists the results of tests conducted for samples of a 3% Ni/Al_2O_3 during the last quarter in the chronological order in which the experiments were performed. The alphabetic suffix indicates test performed on a given catalyst sample. These runs were all performed using the new all glass apparatus described in an earlier report (7). The differences evident in the data collected from different catalyst samples are thought to represent small variations in catalyst properties from sample to sample. These differences may be attributed to such factors as reduction time, heating rate during reduction, the number of times the catalyst was passivated in air and other factors. Each of these factors was carefully watched to insure uniformity, but some small differences are inevitable due to equipment limitations and experimental error.

These results substantiate those of earlier reports, that $Ni(CO)_4$ is formed at 298 K on unpoisoned catalysts in agreement with earlier work by Milliams et al. (8).

A marked increase in CO uptake after poisoning is evident. Indeed, it is apparently a factor of 4 to 10 larger than the uptake of the same sample before poisoning. At the same time the hydrogen uptake for these same samples is seen to decrease upon poisoning. These results agree qualitatively with those obtained earlier with nickel and nickel bimetallic catalysts at 190 K (3). This behavior suggests several possibilities. Sulfur has been shown to act as a catalyst in the formation of $Ni(CO)_4$ (8). However, a decreased amount of material (presumably nickel or some nickel sulfide or carbide) was collected in the heated tube after CO adsorption on the presulfided sample. Presumably more not less nickel would be collected if the formation of $Ni(CO)_4$ were increased by sulfur. Nevertheless, the large values of CO/H (for irreversibly adsorbed CO) could only be explained by a migration of $Ni(CO)_4$ to the support where it decomposes to form strongly bound subcarbonyl nickel species. Another possibility is that the sulfur alters the chemisorptive properties of the CO, causing a greater uptake per surface site in accordance with previous IR studies (9,10). A third possibility is the formation of $(CO)_xS$ species, although no COS was obtained via sulfur analysis. More testing will be needed to explain this phenomenon.

The data in Table 4 suggest that CO adsorption is very sensitive to pretreatment and adsorption temperature. For example, comparison between Runs 26G and 27G shows that a second CO adsorption measurement on the presulfided catalyst at the same temperature was lower than the first. Between runs, the sample was rereduced 1 hour, evacuated and titrated. The difference in the uptake is presumably a result of surface modifications during the first adsorption. Furthermore, on comparing samples 32H and 33H a much greater decrease is revealed when the second measurement is performed at 273 K. In the latter case, the intermediate treatment was nearly the same as for runs 26G and 27G with the difference being that after run 32H, the sample was

Table 4

Comparison of Carbon Monoxide Chemisorption Measurements versus Temperature of Adsorption (3% Ni/Al_2O_3)

Run #	Temp K	Absorbate Gas	Uptake	CO/H	Sulfur poisoned[a]	Ni from Ni(CO)4 Decomposition
22 G	300	H_2	50			
23 G	299	CO	172	1.7		yes
24 G						
25 G	298	H_2	26		yes	
26 G	189	CO	601	11.8[b]	yes	c
27 G	189	CO	500	9.8[b]	yes	d
28 H	298	H_2	49			
29 H	299	CO	133	1.4		yes
30 H						
31 H	298	H_2	23		yes	
32 H	298	CO	796	17.4[b]	yes	d
33 H	273	CO	253	5.6[b]	yes	e

[a] Sample poisoned at around 725 ± 5 K in 10 ppm H_2S in H_2 until approximately 1/2 of the sites were covered. The flow rate of the 10 ppm H_2S mix was 280-300 cm^3/min.

[b] The ratios are calculated on the basis of the H_2 uptake for the poisoned catalyst.

[c] No Ni or sulfur data obtained.

[d] Uncertain residue in heated tube--not readily apparent as to identity -- presently being analyzed.

[e] This sample was passivated between runs due to a problem with the sample cell.

passivated and then rereduced 2 hours. The latter decrease in CO uptake may indicate that less $Ni(CO)_4$ is formed on the sulfided nickel at the lower temperature, again consistent with Milliams et al. (8).

Work in the next quarter in this area will further focus on the differences in chemisorption behavior between fresh and sulfided catalyst.

4. Electron Microscopy

Electron micrographs were taken of Ni-S-101 (13.5% Ni/SiO_2) before and after sintering at 973 K for 54 h and of the silica support. Figure 2 shows a micrograph of fresh Ni-S-101, Figure 3 a micrograph of sintered Ni-S-101, and Figure 4 a micrograph of the silica support.

The Ni crystallites were easily identified and a crystallite size distribution was obtained for both the fresh and sintered samples. For each sample 1200-1300 particles were counted to determine the average crystallite size. Crystallite size distributions are listed in Table 5.

The particle size distribution of the fresh Ni-S-101 sample was quite narrow with an average crystallite diameter of 2.9 nm in very good agreement with estimates from H_2 adsorption. Upon sintering, the distribution became more random with two main peaks. The first occurred at the original particle size and a second at 5.1 to 6.0 nm. This result is reasonable, as the catalyst after sintering for this period of time was not completely deactivated for methanation (11). The average particle size increased by a factor of two, from 2.9 nm to 6.4 nm.

Particle size distributions were much more easily obtained with the Ni-silica samples than with the Ni-alumina samples because in the former case the Ni was much more easily differentiated from the support.

Task 2: Activity and Support Geometry Tests

An activity test of a supported, borohydride reduced Ni catalyst was performed during the past quarter. Data for the Ni boride/Al_2O_3 are compared with those for 14% Ni/Al_2O_3 in Table 6. The results indicate that the nickel boride is more active on a mass basis but slightly less active on a turnover number basis. Methane yields are quite comparable. Further details concerning activity/selectivity and physical properties of metal boride catalysts will soon be available in an M.S. Thesis currently in preparation by Mr. Arthur Uken.

A Ni-impregnated alumina monolith (Ni-AM-203) was activity tested before and after powdering to determine if support geometry (i.e. mass and heat transfer effects) influenced rates and turnover numbers The conditions for the test were 140 kPa, 500 or 525 K, and GHSV = 50,000 h^{-1} with a reactant gas containing 95% N_2, 4% H_2, and 1% CO. Data for these tests reported in Table 6 suggest that support

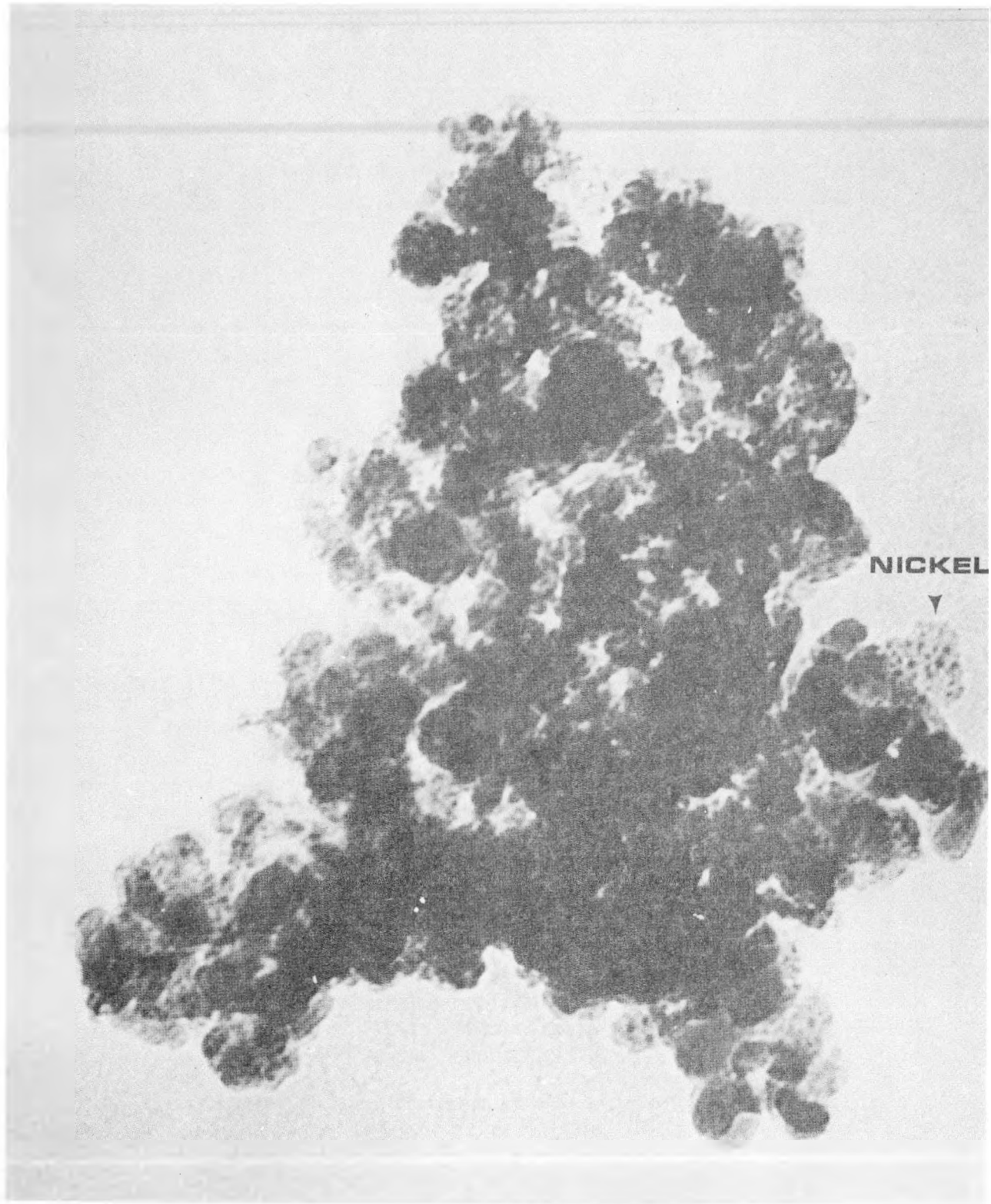

Figure 2. Electron Micrograph of Ni-S-101 (13.5% Ni/SiO_2) Before Sintering.

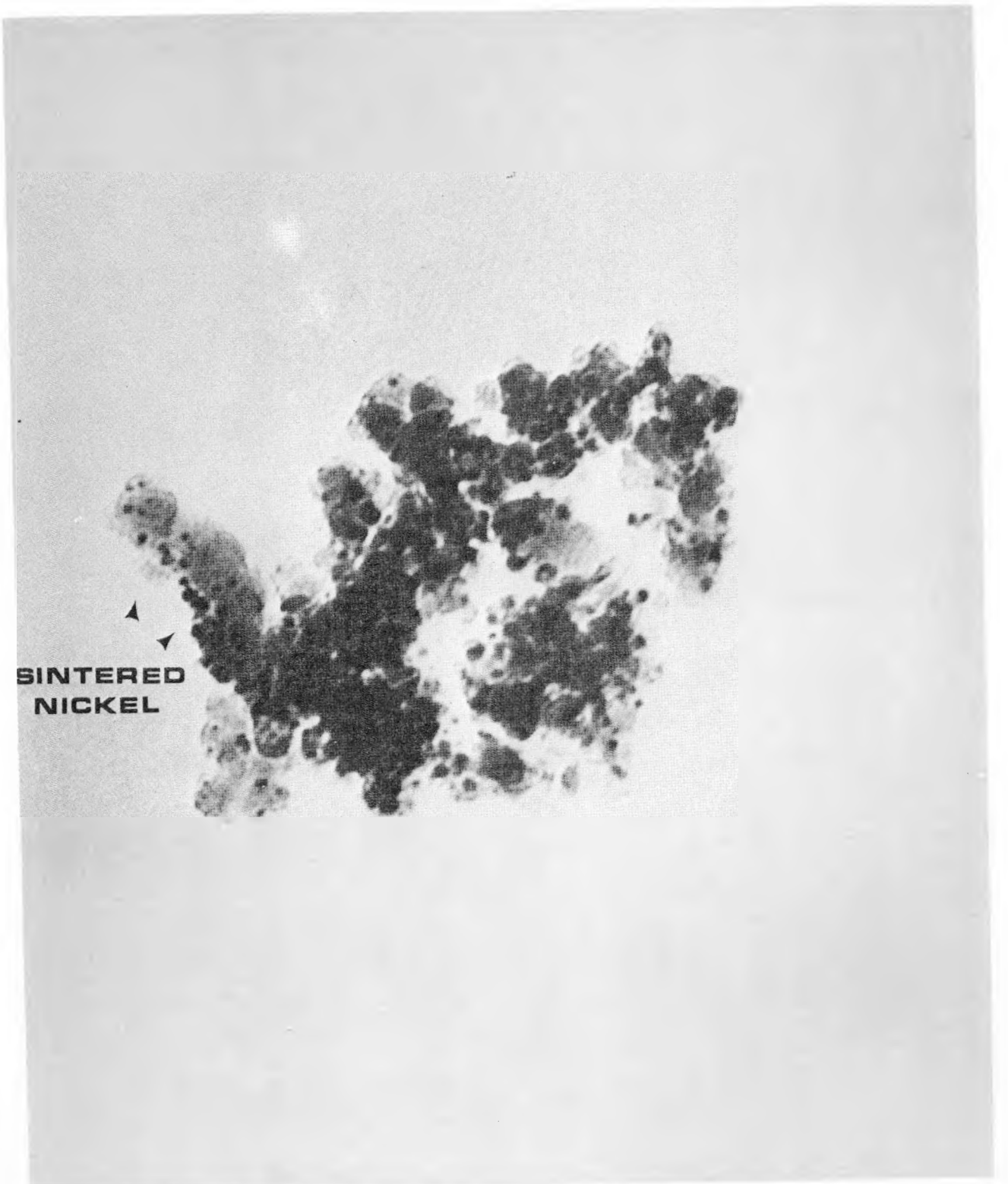

Figure 3. Electron Micrograph of Ni-S-101 (13.5% Ni/SiO_2) After Sintering in H_2 at 973 K for 54 h.

Figure 4. Electron Micrograph of Silica Support.

Table 5

Particle Size Distribution
for Ni-S-101
Fresh and Sintered

% Particles in each size range (n.m.)

Sample	<1	1.1 - 2.0	2.1 - 3.0	3.1 - 4.0
Ni-S-101 Fresh	0	7.8	79.7	10.4

4.1 - 5.0	51 - 60	6.1>
1.1	1.0	0

Average Particle Size: 2.9 n.m.

Ni-S-101 Sintered (700°C)	< 3	3.1 - 4.0	4.1 - 5.0	5.1 - 6.0
	25.1	15.5	8.7	27.4

6.1 - 7.0	7.1 - 8.0	8.1 - 9.0	9.1 - 10.0
8.3	5.4	6.2	1.5

10.1 - 11.0	11.1>
1.3	0.6

Average Particle Size: 6.4 n.m.

Table 6

Activity Test of Borohydride Reduced Nickel Catalyst and Monolith Before and After Powdering

Catalyst	R_{CH_4} ($\times 10^6$)[a]	N_{CH_4} ($\times 10^3$)[b]	% CH_4 Yield[c]
Temperature 523 K			
Ni-B-A-105[d]	26.6	4.1	82
Ni-A-116[e]	20.5	6.3	77
Temperature 500 K			
Ni-AM-203 (whole)[f]	1.1	3.0	79
Ni-AM-203 (Powdered)	0.91	2.5	72
Temperature 525 K			
Ni-AM-203 (whole)	2.7	7.4	89
Ni-AM-203 (Powdered)	2.6	7.4	85

[a] Rate of methane production per gram catalyst per second.

[b] Methane turnover number based on H_2 adsorption at 300 K in units of molecules CH_4 per site per second.

[c] Fraction of converted CO which becomes methane.

[d] Borohydride reduced; dried in flow H_2.

[e] Previously reported.

[f] After testing the monolith whole it was crushed to a powder and tested again.

geometry does not influence rates and turnover numbers at low conversions, since at 500 and 525 K there is little difference in rates/g and turnover number for the monolith and its powder. Thus, the higher turnover numbers and rates observed previously (3) for monolith compared to pelleted catalyst are probably due to particle size effects, preparation techniques, or support-metal interactions.

Task 3: Kinetic Studies

It was also found that our mass flows are more pressure sensitive than previously thought. Calibrations of the flow meter were made for the three pressures mentioned above. Changes were also made in the plumbing to minimize the total volume of the system in order to reduce the time required to reach steady state at high pressures.

Kinetic tests were made on four 3% nickel monolithic catalysts. The first two tests were made at 473 K and 3 pressures, 690, 3450, 6900 kPa on Ni-M-157 and Ni-M-158. At this low temperature, both catalysts deactivated. Further studies will attempt to discern the reason for this deactivation.

Ni-M-184 was studied extensively during this quarter. In fact over 100 hours of reactor experiments were performed at 70 different conditions of temperature, pressure and feed gas composition. Tables 7, 8, and 9 show some of the data and results of this test. Since reaction rates in a stirred tank reactor are dependent on product composition, product mole fractions are reported instead of feed composition. In these tests, space velocities were generally held constant while conversions were allowed to vary. At these high pressures and low temperatures, the expected increase in reaction rate with increased pressure does not appear. The effect of increasing pressure on the methanation reaction rates changes with temperature. At 498 K, the rate decreases; at 523 K no significant change occurs; and at 548 K, the rate increases. The methane yield also increases with increasing temperature and decreases with increasing pressure. Extrapolation of methane yield with pressure gives yields comparable with those measured at atmospheric pressure. At lower temperatures, higher pressures apparently favor wax or higher hydrocarbon formation. Some deactivation occurred during the test. This is attributed to a failure in the mole sieve trap allowing mole sieve dust into the reactor and on the catalyst. Wax or carbide formation may have also contributed to the deactivation.

A fourth test was made on Ni-M-183. Nitrogen, for economical reasons, replaced argon as the diluent. Kinetics were measured at 498 and 523 K. Since reaction rates in a stirred tank reactor are dependent on product composition, efforts were made in this test to control product compositions by varying the space velocity. This enabled us to hold one of reactant's concentration constant while varying the other reactant. The results for this test are reported in Tables 10 and 11. While the data in this test seem more consistent, the measured reaction rates are comparable to those measured for Ni-M-184. The effects of temperature and pressures on the reaction rates

Table 7

Kinetic Data for Ni-M-184 at 498 K

Pressure	Product Mole Fraction x 100 CO	H_2	Space Velocity x 10^{-3}	X_{CO} %	R_{CO}[a] µmoles/g-sec	R_{CH_4}[b] µmoles/g-sec	Yield CH_4[c] %
690	1.275	5.70	15	15.0	0.62	0.27	43.7
	0.829	3.75	15	17.1	0.47	0.23	49.5
	0.878	1.86	15	12.2	0.34	0.13	37.9
	2.622	5.81	15	6.3	0.52	0.17	33.0
	1.831	5.77	15	8.5	0.46	0.21	44.3
	0.870	2.82	15	13.0	0.36	0.17	47.2
3450	0.528	2.73	15	29.7	0.61	0.25	40.2
	0.771	3.67	15	22.9	0.63	0.28	47.3
	0.807	2.78	15	19.3	0.53	0.10	38.3
	0.840	1.85	15	16.0	0.44	0.14	30.6
	1.330	2.24	15	11.3	0.47	0.15	31.1
6900	0.559	2.75	15	25.4	0.56	0.23	43.1
	0.810	3.75	15	19.0	0.52	0.23	43.4
	0.841	2.82	15	15.9	0.44	0.16	36.8
	0.883	1.85	15	11.7	0.32	0.13	40.6
	1.306	2.82	15	12.9	0.53	0.16	30.5

[a] [b] Rate of CO conversion per gram catalyst per second.
[c] Rate of CH_4 production per gram catalyst per second.
Percent of converted CO appearing as CH_4.

Table 8

Kinetic Data for Ni-M-184 at 523 K

Pressure	Product Mole Fraction x 100 CO	H_2	Space Velocity x 10^{-3}	X_{CO} %	R_{CO}[a] µmoles/g-sec	R_{CH_4}[b] µmoles/g-sec	Yield CH_4[c] %
690	0.572	2.64	30	23.8	0.98	0.66	66.9
	0.803	3.62	30	19.7	1.09	0.70	64.5
	0.834	2.68	30	16.6	0.91	0.59	64.7
	0.870	1.76	30	13.0	0.72	0.45	62.3
	1.338	2.74	30	10.8	0.89	0.48	53.6
3450	0.483	2.58	30	35.6	1.47	0.78	53.0
	0.767	3.52	30	29.6	1.63	0.87	53.6
	0.730	2.61	30	27.1	1.49	0.72	48.5
	0.777	1.73	30	22.3	1.23	0.49	39.9
	1.237	2.69	30	17.5	1.45	0.56	38.9
6900	0.466	2.56	30	37.9	1.57	0.81	52.0
	0.695	3.51	30	30.5	1.68	0.89	53.3
	0.742	2.64	30	25.9	1.43	0.67	46.8
	0.787	1.75	30	21.3	1.18	0.46	38.8
	1.251	2.74	30	16.6	1.37	0.48	34.8

[a] Rate of CO conversion per gram catalyst per second.
[b] Rate of CH_4 production per gram catalyst per second.
[c] Percent of converted CO appearing as CH_4.

Table 9

Kinetic Tests for Ni-M-184 at 548 K

Pressure	Product Mole Fraction x 100 CO	Product Mole Fraction x 100 H_2	Space Velocity x 10^{-3}	X_{CO} %	R_{CO}[a] µmoles/g-sec	R_{CH_4}[b] µmoles/g-sec	Yield CH_4[c] %
690	0.593	2.71	100	20.9	2.88	1.77	61.5
	0.868	3.70	100	13.2	2.42	1.82	75.3
	0.876	2.73	100	12.4	2.28	1.65	72.5
	0.897	1.80	100	10.3	1.89	1.19	63.0
	1.354	2.69	75	9.71	2.00	1.41	70.3
3450	0.577	2.67	100	22.9	3.15	2.01	63.8
	0.808	3.63	100	19.2	3.53	2.26	63.9
	0.835	2.66	100	16.5	3.03	1.92	63.4
	0.873	1.78	100	12.8	2.34	1.34	57.3
	1.276	2.64	75	14.9	3.09	1.65	53.5
6900	0.427	2.35	75	43.1	4.44	2.99	67.3
	0.601	3.21	75	39.9	5.50	3.67	66.0
	0.686	2.43	75	31.4	4.33	2.60	52.6
	0.693	1.52	60	30.7	3.38	1.78	52.6
	1.125	2.47	60	25.0	4.13	1.96	47.4

[a] Rate of CO conversion per gram catalyst per second.
[b] Rate of CH_4 production per gram catalyst per second.
[c] Percent of converted CO appearing as CH_4.

Table 10

Kinetic Data for Ni-M-183 at 498 K

Pressure	Product Mole Fraction x 100 CO	H_2	Space Velocity x 10^{-3}	X_{CO} %	R_{CO}[a] µmoles/g-sec	R_{CH_4}[b] µmoles/g-sec	Yield CH_4[c] %
690	0.641	2.73	16	17.9	0.40	0.26	65.2
	0.855	3.67	18	13.5	0.45	0.24	58.7
	0.894	2.64	15	12.6	0.35	0.18	51.4
	0.878	1.82	12	9.8	0.22	0.12	53.5
	1.364	2.74	13	8.4	0.30	0.12	38.0
3450	0.618	2.73	22	14.9	0.45	0.21	47.0
	0.868	3.76	26	14.7	0.71	0.23	32.7
	0.877	2.71	22	11.8	0.29	0.17	37.7
	0.904	1.80	18	12.4	0.41	0.11	26.9
	1.378	2.74	19	9.4	0.50	0.14	28.0
6900	0.644	2.78	19	14.4	0.38	0.20	53.0
	0.877	3.72	21	12.6	0.49	0.24	49.0
	0.895	2.79	18	10.8	0.36	0.14	39.9
	0.915	1.88	15	8.7	0.24	0.08	31.6
	1.383	2.67	15	8.2	0.34	0.10	28.1

[a] Rate of CO conversion per gram catalyst per second.
[b] Rate of CH_4 production per gram catalyst per second.
[c] Percent of converted CO appearing as CH_4.

Table 11

Kinetic Data for Ni-M-183 at 523 K

Pressure	Product Mole Fraction x 100 CO	H_2	Space Velocity x 10^{-3}	X_{CO} %	R_{CO}[a] µmoles/g-sec	R_{CH_4}[b] µmoles/g-sec	Yield CH_4[c] %
690	0.629	2.66	53	16.4	1.21	0.97	80.2
	0.888	3.70	68	11.5	1.45	1.03	71.0
	0.879	2.65	50	12.4	1.15	0.85	74.1
	0.884	1.73	40	11.9	0.88	0.65	73.7
	1.356	2.68	40	8.97	1.00	0.66	66.3
3450	0.621	2.61	75	17.4	1.82	1.21	66.3
	0.875	3.66	92	12.9	2.19	1.36	62.2
	0.864	2.55	70	14.1	1.83	1.02	56.1
	0.873	1.69	57	13.0	1.38	0.70	51.0
	1.351	2.69	57	10.3	1.63	0.74	45.7
6900	0.642	2.73	90	14.7	1.83	1.06	57.8
	0.893	3.86	105	10.9	2.12	1.16	54.6
	0.893	2.70	85	11.0	1.74	0.88	50.9
	0.885	1.62	68	11.9	1.50	0.68	45.4
	1.372	2.62	71	8.94	1.86	0.76	43.5

[a]Rate of CO conversion per gram catalyst per second.
[b]Rate of CH_4 production per gram catalyst per second.
[c]Percent of converted CO appearing as CH_4.

found in the testing of Ni-M-184 are confirmed. A power law rate equation of the form $r = (A) \exp[-E/R] (CO)^X (H_2)^Y$ was used to fit the data. The activation energy is approximately 114 kJ while the values for X and Y vary from -1 to -0.4 and 1 to 0.6 respectively, the results of the rate equation calculation are compiled in Table 12.

Tests in the next quarter will include a high pressure, low temperature deactivation test, kinetic studies at higher temperatures and lower metal loadings, and a comparison of pellets with monoliths.

During the past quarter several kinetic experiments were performed in the Quartz mixed flow reactor. The conditions for the low pressure kinetics were 103 kPa, 550 K and GHSV = 40,000 h^{-1}. Concentration of CO was varied from 1 to 3 mole % and concentration of H_2 was varied from 2 to 20 mole %. The balance of the reactant gas was argon. As pointed out by Berty (12) the impeller in the quartz reactor designed by Katzer and Fitzharris (4) produces very little pressure head. Thus, only a thin layer of catalyst can be studied without non-idealities arising. For the kinetics tests and subsequent H_2S poisoning tests 0.1 g of catalyst sample was spread in a thin layer in the catalyst basket. The catalyst sample was ground and sieved to -60 + 120 mesh.

In a mixed flow reactor the reaction rate is measured at the outlet concentration. Thus, inlet H_2/CO ratios and concentrations may vary if conversions are high. Table 13 shows the orders of reaction obtained for CO and H_2. For these kinetic tests efforts were made to keep conversions low (below 10%). For the tests measuring the exponent of P_{CO} this was possible. However, for the tests measuring the exponent of P_{H_2}, carbon monoxide conversions as high as 30% were obtained. So, there is less confidence in the value of Y. However, our data compare well with those of Vannice for Ni on Al_2O_3 (13).

After partial *in situ* poisoning with H_2S, kinetics for methanation were remeasured for a Ni-A-120 sample. While X and Y are slightly lower than in the unpoisoned case, there appears to be no significant change in the orders of reaction. This supports the idea that sulfur poisoning is mainly a blockage or covering of the active nickel surface.

Task 4: Degradation Studies

Long term H_2S poisoning tests were performed on Ni-A-120 (3% Ni) samples in the Quartz CFSTR described previously (4,6). For all of these tests the conditions were 103 kPa, 550 or 575 K, GHSV = 40,000 h^{-1} and reactant gas mixture containing 79% Ar, 20% H_2 and 1% CO with 1 ppm H_2S. The H_2/CO ratio was 20/1 and P_{H_2S}/P_{H_2} ratio was 5×10^{-6}. Thus, the partial pressure of H_2S in these experiments should be well below the bulk sulfide forming region (14). Activity versus time curves are shown in Figure 5 for two samples. The first one run is the -60 mesh powder. The activity dropped off rapidly and somewhat erratically within the first five hours. This rapid decrease may be due to switching the reactant gas tanks at time zero. This procedure may have allowed air to contact the sample if the regulator and line were not sufficiently purged. This problem was eliminated

Table 12

Orders of Methanation[a]
for Ni-M-183

Pressure	X	Y
T = 498 K		
690	-1.07	1.11
3450	-1.03	1.13
6900	-1.02	0.97
T = 523 K		
690	-0.44	0.60
3450	-0.57	0.86
6900	-0.67	0.77

Activation Energies

Pressure	E (kJ/mole)
690	-114
3450	-110
6900	-118

[a] $r = A\, e^{-E/RT}\, P_{CO}^{X}\, P_{H_2}^{Y}$

Table 13

Methanation Kinetics at Low Pressure

Catalyst	X[a]	Y[a]
Ni-A-120 Before Poisoning	-0.28	0.91
Ni-A-120 After Poisoning	-0.38	0.79
Ni/Al_2O_3[b]	-0.3	0.8

[a] According to the rate expression $R_{CH_4} = k\ P_{CO}^{X}\ P_{H_2}^{Y}$

[b] Reported by Vannice (13).

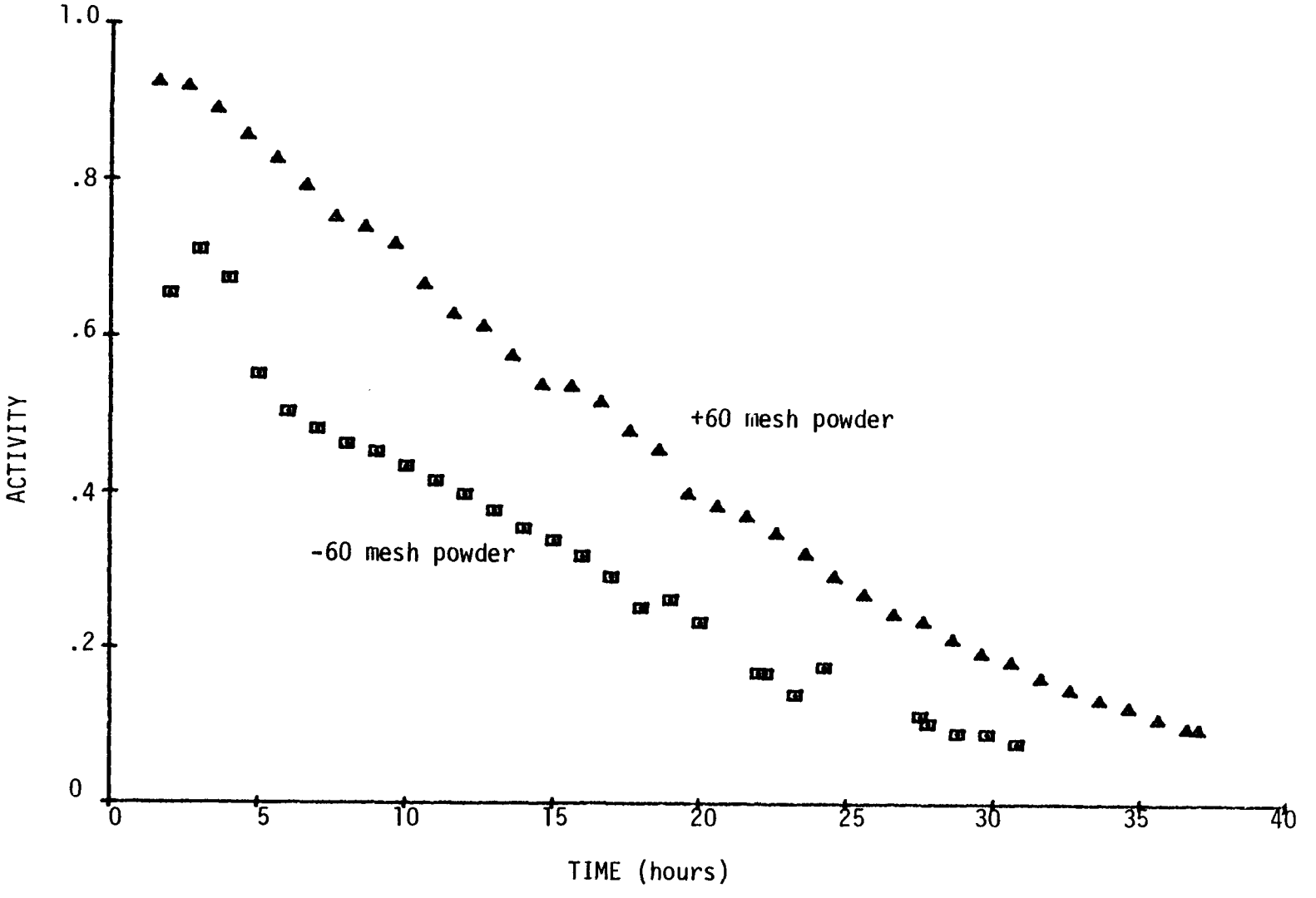

Figure 5: Activity versus Time plot of H_2S Poisoning *In situ* of Ni-A-120 Powders in a Quartz CFSTR at 550 K, 103 kPa, and reactant gas containing 79% Ar, 20% H_2, 1% CO and 1 ppm H_2S.

in subsequent tests. Instead, 79% Ar, 10% H_2 and 1% CO gas tank mixture was added with a pure H_2 stream to make a 20/1 H_2/CO reactant mixture. At time zero the pure H_2 stream was replaced with H_2S in H_2 to make a 20/1 H_2/CO reactant mixture with 1 ppm H_2S. For the second set of data shown in Figure 5, the latter procedure was used and the initial deactivation was more gradual. The deactivation is almost straight line even though this sample is a coarse powder (+60 mesh). There is some tailing off near the end of the run.

In Appendix A we derive a kinetic model for linearizing H_2S deactivation data to find k_d, the deactivation rate constant. A plot of $\ln (P_{CO_0} - P_{CO}/P_{CO}^{.63})$ versus time should yield a straight line. In Figure 6 the data for the +60 mesh and the -60 + 120 mesh powdered catalysts are shown. Both powders are nickel supported on a high surface area alumina. The finer powder gave a good fit to a straight line. However, for the coarser powder the fit was not as good. This may be because sulfur poisoning is pore diffusion limited and gives different rates for different catalyst powder sizes. Also, during the test with the +60 mesh powder carbon deposit on the inlet tube to the reactor appeared. Since the tube is made of quartz, the carbon deposit was most likely due to decomposition of $Fe(CO)_5$. This may also have caused the more rapid deactivation of this catalyst. The mole sieve filter was baked out after this run to remove impurities. For the subsequent tests no carbon buildup was found on the inlet tube.

Further H_2S long term poisoning runs were performed on Ni-A-120, -60 + 120 mesh powder. A graph of $\ln (P_{CO_0} - P_{CO}/P_{CO}^{.63})$ versus time is shown in Figure 7. These tests were performed at 550 and 575 K. In this case the data do not fit a straight line very well, suggesting that the linearization derived in Appendix A is not the proper model for H_2S poisoning. In Figure 8, plots of activity versus time are shown. These plots give a better fit to a straight line. This may be explained if H_2S poisoning is essentially zero order in activity and H_2S merely blocks nickel surface sites.

At 1 ppm H_2S it would take about 13 to 16 hours for H_2S to completely cover the nickel surface assuming a S/H adsorption ratio of 0.8 (7) and all the sulfur adsorbs. Both tests were terminated before 16 hours. However, in each case the catalysts retained some of their original activity, suggesting that all the H_2S was not adsorbed on the catalyst. Because the teflon sampling valve for H_2S detection by FPD was not working, no data on the outlet concentration of H_2S is shown. Ths valve will be fixed so that outlet H_2S data can be correlated with activity data in future runs.

Deactivation rate constants for the H_2S poisoning runs were calculated using both the linearizing formula from Appendix A and the activity versus time plots. These are shown in Table 14. Data from runs A and B are suspect because of problems with reactant gas flow and/or carbon deposition. However, the data in Runs C and D are believed to be representative and hence apparent activation energies were calculated for Runs C and D. Further work will be done during the next quarter to try to determine a more general, quantitative

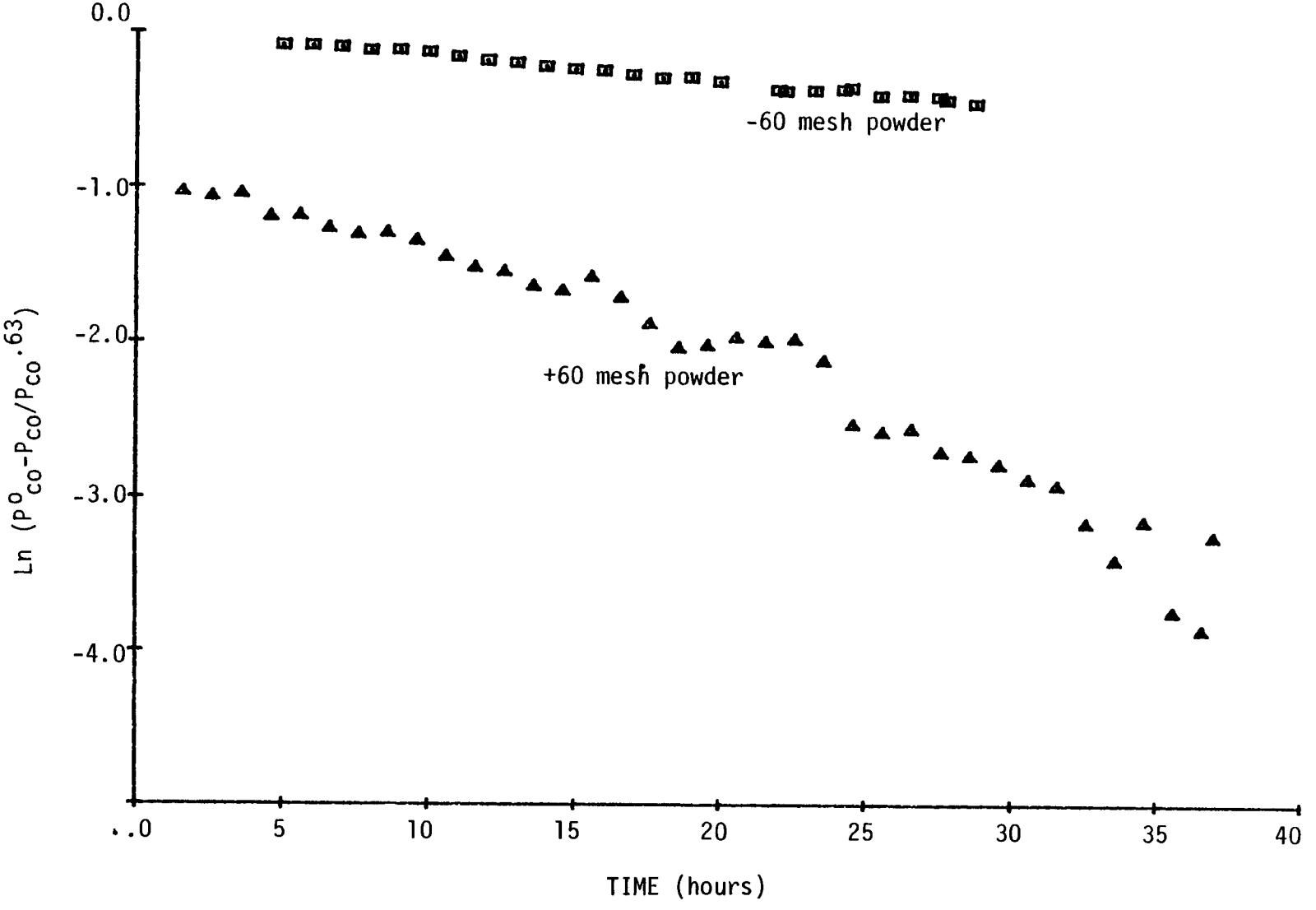

Figure 6: Linearized Plot of H_2S Poisoning In situ of Ni-A-120 Powders in a Quartz CFSTR at 550 K, 103 kPa, and reactant gas containing 79% Ar, 20% H_2, 1% CO and 1 ppm H_2S.

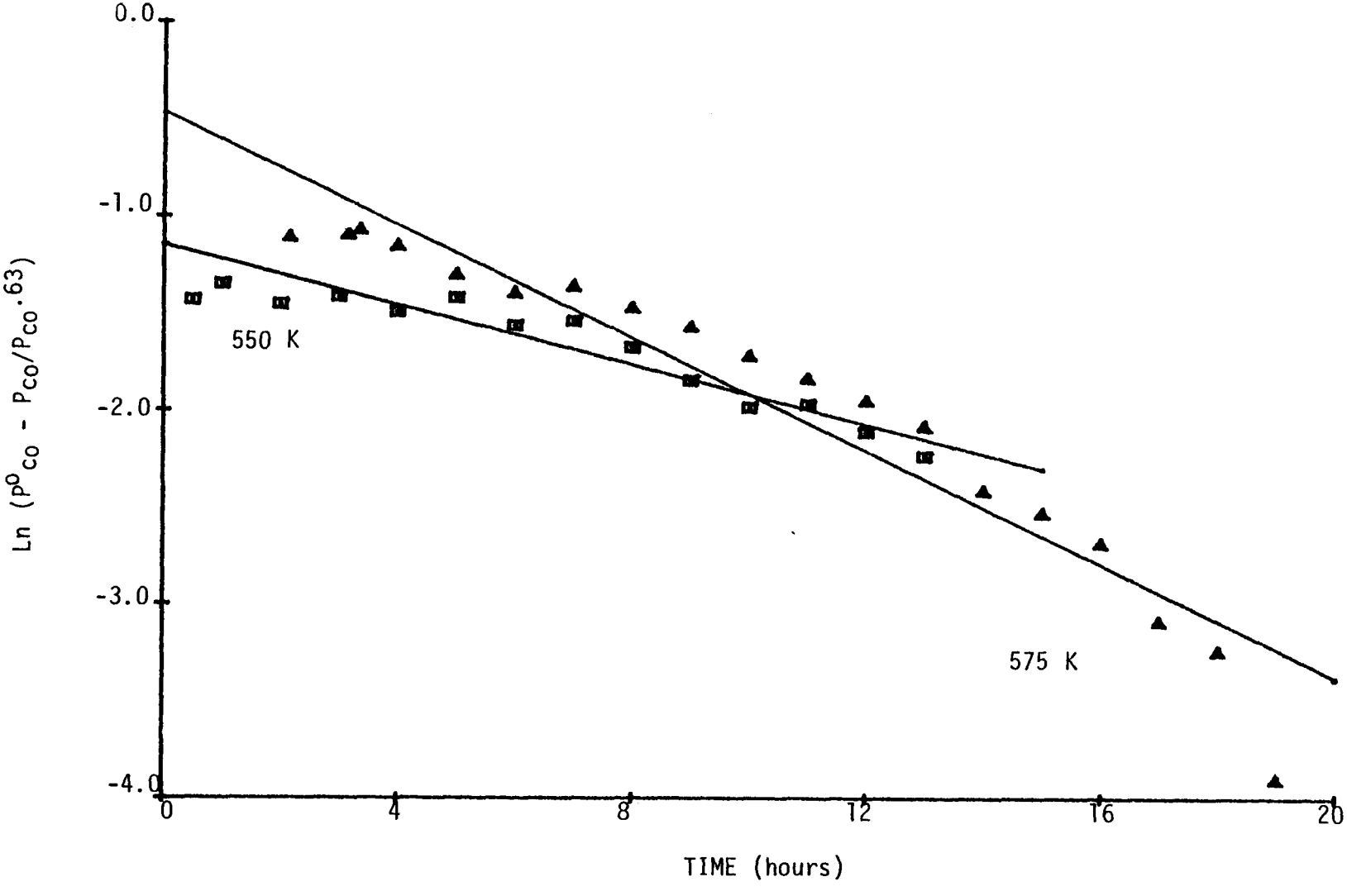

Figure 7: Linearized Plot of H_2S poisoning In situ of Ni-A-120 -60+120 mesh Powder at 550 and 575 K, 103 kPa, and reactant gas containing 79% Ar, 20% H_2, 1% CO and 1 ppm H_2S.

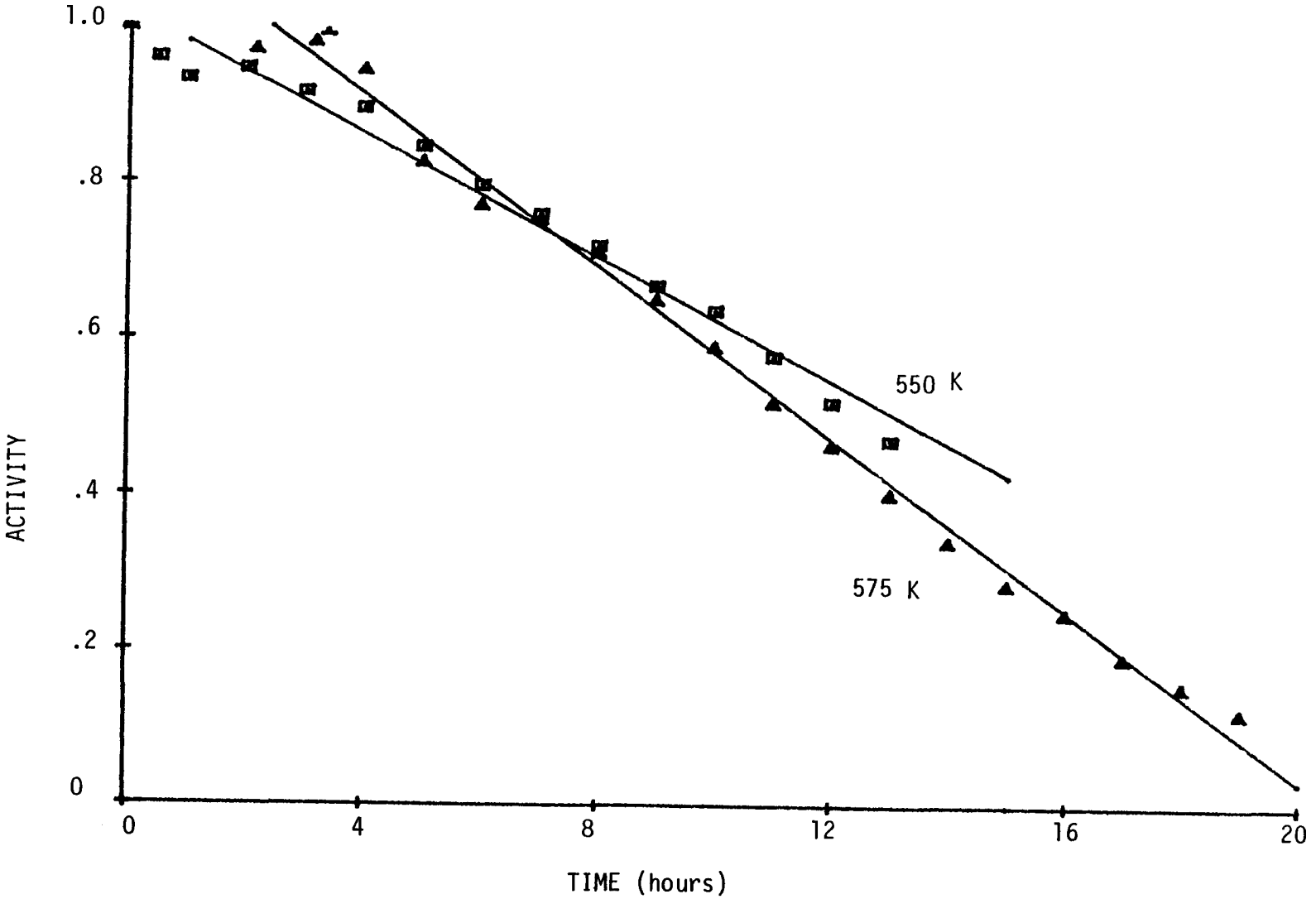

Figure 8: Activity versus Time Plot of H_2S Poisoning In situ of Ni-A-120 -60+120 mesh powder at 550 and 575 K, 103 kPa, and reactant gas containing 79% Ar, 20% H_2, 1% CO and 1 ppm H_2S.

Table 14

H_2S Deactivation Rate Constants
for Ni-A-120 Powder

Catalyst	Run	Temperature of deactivation	k_d [a]	k_d [b]
-60 + 120 mesh	A	550 K	0.016[a]	0.018[c]
+60 mesh	B	550 K	0.069[d]	0.025[d]
-60 + 120 mesh	C	550 K	0.072	0.040
-60 + 120 mesh	D	575 K	0.15	0.055
Apparent Activation Energies from runs C and D			16,100 cal/gmole	8,300 cal/gmole

[a] Deactivation rate constant calculated from formula in Appendix A.

[b] Deactivation rate constant assuming zero order deactivation.

[c] These data are suspect because of problems with the reactant gas flow.

[e] These data are suspect since carbon deposits appeared on the inlet tube.

model for H_2S poisoning and the effect of H_2S concentration on deactivation.

Task 5: Technical Interaction and Technology Transfer

This quarter included numerous technical communications by phone, mail, and visits with other workers in catalysis.

During the first week in April, the principal investigator was asked by Mr. Roger Billings of Billings Energy Corp. to join with a group of local engineers and scientists in a round-the-clock effort to provide assistance to DOE in removing the H_2 bubble from the Three-Mile Nuclear Reactor. Dr. Bartholomew was assigned to find colloidal catalysts which would catalyze the reaction of H_2 with O_2 or other oxidizing agents in aqueous solution. It was determined that borohydride reduced Pt worked whereas Ni didn't.

During the quarter our laboratory received requests from Conoco and Northwest Battelle to supply methanation catalysts for long term testing. Catalysts were sent to Battelle to be tested in their process which converts cellulose to methane. We are making arrangements to supply Conoco with the appropriate catalysts.

Dr. Bartholomew recently interacted closely with other workers at SRI International, IGT and the University of Delaware in regard to sulfur poisoning of methanation catalysts. During a visit to IGT on June 13th, he discussed industrial requirements for sulfur tolerant catalysts with Mr. Tony Lee.

On June 22, the PI visited the Chemicals Division of Ventron in Beverly, Mass. where he presented a seminar on "Borohydride Reduced Catalysts in Hydrogenation of CO."

The following week (June 24-28) he attended the Gordon Conference on Catalysis in New London, New Hampshire where he presented a similar talk on Metal Boride Methanation Catalysts. Since, the conference emphasized Fischer-Tropsch and Methanation studies, it was quite pertinent to the work in our laboratory. A number of speakers presented evidence for an active carbon intermediate in methanation and Fischer-Tropsch synthesis, in accord with some of our own studies supported by NSF.

On June 29-30, Dr. Bartholomew visited Professor James Katzer at the University of Delaware where he toured facilities in the new Center for Catalytic Science and Technology and discussed methanation and sulfur poisoning work.

During the quarter a publication dealing with sulfur poisoning of nickel based on work supported by this contract was accepted for publication by the Journal of Catalysis. Several other publications including three directly related to this contract are in various stages of preparation.

Mr. Paul Moote joined our research group in June and is assisting Monsieurs Erekson and Sughrue in their kinetic and poisoning studies.

IV. CONCLUSIONS

1. Monolithic catalysts can be prepared with metal dispersions equivalent to those obtained with pellets in the low metal loading regime (0.5-5 wt. metal).

2. CO adsorption on Ni/Al_2O_3 at 273 and 298 K increases by 300-800% after partial presulfiding with 10 ppm H_2S just as it did for CO adsorption on Ni/Al_2O_3 at 190 K.

3. Very good agreement is observed for the metal crystallite diameters in a 13.5% Ni/SiO_2 measured by Electron Microscopy and H_2 adsorption (assuming $H/Ni_s = 1$).

4. A borohydride reduced Ni_2B/Al_2O_3 appears to have approximately the same methanation activity as Ni/Al_2O_3 of equivalent loading and surface area.

5. A crushed and uncrushed sample of the same monolithic nickel catalyst show the same intrinsic specific activity within experimental error. Hence the geometry of the catalyst doesn't appear to influence our determination of intrinsic catalytic activity.

6. Kinetic measurements over a range of temperatures (200-275 K) and pressure (8-75 atm) result in kinetic parameters very similar to those determined at 1 atm and 200-250 K. However, reaction orders of H_2 and CO vary significantly with temperature and pressure.

7. The kinetics of deactivation of nickel catalysts by H_2S during methanation reaction can be modelled fairly well by a Levenspiel type deactivation model.

V. REFERENCES

1. M. Greyson, "Methanation" in "Catalysts" Vol. IV., ed. P.H. Emmett, Rheinhold Pub. Corp., New York (1956).

2. G.A. Mills and F.W. Steffgen, "Catalytic Methanation," Catalysis Reviews 8, 159 (1973).

3. C.H. Bartholomew, "Alloy Catalysts with Monolith Supports for Methanation of Coal-Derived Gases," Final Technical Progress Report FE-1790-9 (DOE), (Sept. 6, 1977).

4. W.D. Fitzharris and J.R. Katzer, Ind. Eng. Chem. Fundam. 17, 130 (1978).

5. J.L. Oliphant, R.W. Fowler, R.B. Pannell and C.H. Bartholomew, "Chemisorption of Hydrogen Sulfide on Nickel and Ruthenium Catalysts, I. Desorption Isotherms," J. Catal. 51, 229 (1978).

6. C.H. Bartholomew, "Alloy Catalysts with Monolith Supports for Methanation of Coal-Derived Gases," Annual Technical Progress Report FE-2729-4, (DOE), (October 5, 1978).

7. C.H. Bartholomew, "Alloy Catalysts with Monolith Supports for Methanation of Coal-Derived Gases," Quarterly Technical Progress Report FE-2729-5 (DOE), (January 5, 1979).

8. D.E. Milliams, J. Pritchard, and K.W. Sykes, Proceedings of the 6th International Congress on Catalysis, ed. G.C. Bond, P.B. Wells, and F.C. Tompkins, Vol. 1, p. 417 (1977).

9. C.H. Rochester and R.J. Terrell, JCS Faraday I, 73, 609 (1977).

10. R.T. Rewick and H. Wise, J. Phys. Chem. 82, 752 (1978).

11. C.H. Bartholomew, "Kinetic, Adsorption, and Poisoning Studies of Alloy Methanation Catalysts," Annual Report ENG 76-81869 (NSF), (August 15, 1978).

12. J.M. Berty, Ind. Ind. Eng. Chem. Fundam. 18, 193 (1979).

13. M.A. Vannice, J. Catal. 37, 449 (1975).

14. T. Rosenquist, J. of Iron and Steel Inst. 176, 37 (1954).

Appendix A

Model for finding k_d, the deactivation rate constant:

Stirred tank performance equation:

1) $W/F_o = X_{CO}/(-r_{CO})a$

First order deactivation:

2) $-da/dt = k_d a$ (Assume P_{H_2S} is constant and included in k_d.)

Integrating 2.

3) $a = a_o\, e^{-k_d t}$ (let $a_o = 1.0$)

The kinetic expression for methanation from Table 13.

4) $-r_{CO} = kP_{CO}^{-.28}\, P_{H_2}^{.91}$

$P_{H_2} = 20\, P_{CO}$. This expression holds for small conversions in a stirred tank reactor. Substituting:

5) $-r_{CO} = k\, 20^{.91}\, P_{CO}^{.63}$

Conversion equation

6) $X_{CO} = \dfrac{(P^o_{CO}-P_{CO})}{P^o_{CO}}$ (Assume conversions are small. Therefore, the expansion factor is negligible.)

Substituting 3,5 and 6 into 1.

7) $W/F_o = \dfrac{(P^o_{CO} - P_{CO})/P^o_{CO}}{k\, 20^{.91} P_{CO}^{.63}\, e^{-k_d t}}$

Rearranging

8) $e^{-k_d t} = \left(\dfrac{F_o}{W\, P^o_{CO}\, k\, 20^{.91}}\right)\left(\dfrac{P^o_{CO}-P_{CO}}{P_{CO}^{.63}}\right)$

Taking the ln of both sides

9) $\ln\left(\dfrac{P^o_{CO}-P_{CO}}{P_{CO}^{.63}}\right) = -\ln\left(\dfrac{F_o}{W\, P^o_{CO}\, 20^{.91}}\right) - k_d t$

Thus, plotting $\ln\left[\dfrac{P^o_{CO}-P_{CO}}{P_{CO}^{.63}}\right]$ versus time should give a straight line. The slope will be $-k_d$.

Nomenclature for Appendix A

a	activity (rate at any time/rate at initial time)
a_o	activity at initial time, equals 1.0
F_o	molar feed rate of CO
k	methanation rate constant
k_d	deactivation rate constant
P_{CO}	partial pressure of CO
P_{H_2}	partial pressure of H_2
P_{H_2S}	partial pressure of H_2S
$-r_{CO}$	rate of disappearance of CO
t	time
W	weight of catalyst